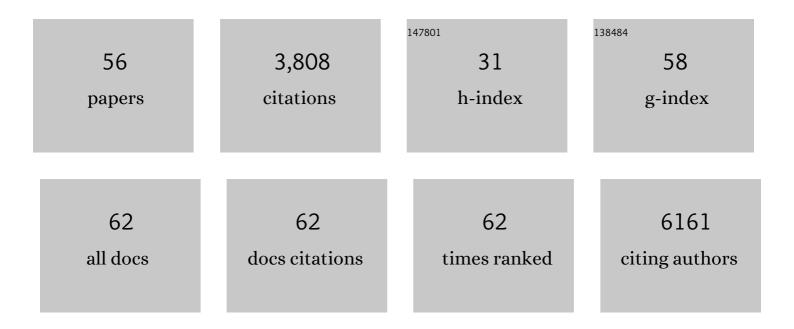
Zhongliang Wang

List of Publications by Year in descending order

Source: https://exaly.com/author-pdf/2101902/publications.pdf Version: 2024-02-01



#	Article	IF	CITATIONS
1	Erythrocyte Membrane Camouflaged Metal–Organic Framework Nanodrugs for Remodeled Tumor Microenvironment and Enhanced Tumor Chemotherapy. Advanced Functional Materials, 2022, 32, 2107791.	14.9	39
2	A metabolic acidity-activatable calcium phosphate probe with fluorescence signal amplification capabilities for non-invasive imaging of tumor malignancy. Science Bulletin, 2022, 67, 288-298.	9.0	11
3	Self-sufficient copper peroxide loaded pKa-tunable nanoparticles for lysosome-mediated chemodynamic therapy. Nano Today, 2022, 42, 101337.	11.9	41
4	GPR125 positively regulates osteoclastogenesis potentially through AKT-NF-κB and MAPK signaling pathways. International Journal of Biological Sciences, 2022, 18, 2392-2405.	6.4	7
5	A Potent Strategy of Combinational Blow Toward Enhanced Cancer Chemoâ€Photodynamic Therapy via Sustainable GSH Elimination. Small, 2022, 18, e2106100.	10.0	18
6	Bioorthogonally activatable cyanine dye with torsion-induced disaggregation for in vivo tumor imaging. Nature Communications, 2022, 13, .	12.8	27
7	Liposome trade-off strategy in mitochondria-targeted NIR-cyanine: balancing blood circulation and cell retention for enhanced anti-tumor phototherapy in vivo. Nano Research, 2021, 14, 2432-2440.	10.4	14
8	Harnessing Hypoxiaâ€Dependent Cyanine Photocages for Inâ€Vivo Precision Drug Release. Angewandte Chemie, 2021, 133, 9639-9647.	2.0	3
9	Harnessing Hypoxiaâ€Dependent Cyanine Photocages for Inâ€Vivo Precision Drug Release. Angewandte Chemie - International Edition, 2021, 60, 9553-9561.	13.8	28
10	Development and Validation of a Nomogram for Preoperative Prediction of Lymph Node Metastasis in Lung Adenocarcinoma Based on Radiomics Signature and Deep Learning Signature. Frontiers in Oncology, 2021, 11, 585942.	2.8	20
11	Recent progress in drug delivery and cancer theranostic built from metal-organic framework. Biomedical Materials (Bristol), 2021, 16, 042011.	3.3	10
12	Estimating dynamic vascular perfusion based on Er-based lanthanide nanoprobes with enhanced down-conversion emission beyond 1500 nm. Theranostics, 2021, 11, 9859-9872.	10.0	6
13	Controllable Coumarin-Based NIR Fluorophores: Selective Subcellular Imaging, Cell Membrane Potential Indication, and Enhanced Photodynamic Therapy. ACS Applied Materials & Interfaces, 2020, 12, 2076-2086.	8.0	37
14	Calming the Cytokine Storm in Pneumonia by Biomimetic Nanoparticles. Matter, 2020, 3, 18-20.	10.0	11
15	Engineering Macrophages for Cancer Immunotherapy and Drug Delivery. Advanced Materials, 2020, 32, e2002054.	21.0	464
16	Innenrücktitelbild: Rabies Virusâ€Inspired Metal–Organic Frameworks (MOFs) for Targeted Imaging and Chemotherapy of Glioma (Angew. Chem. 39/2020). Angewandte Chemie, 2020, 132, 17455-17455.	2.0	0
17	Acidâ€Induced In Vivo Assembly of Gold Nanoparticles for Enhanced Photoacoustic Imagingâ€Guided Photothermal Therapy of Tumors. Advanced Healthcare Materials, 2020, 9, e2000394.	7.6	44
18	Rabies Virusâ€Inspired Metal–Organic Frameworks (MOFs) for Targeted Imaging and Chemotherapy of Glioma. Angewandte Chemie, 2020, 132, 17130-17136.	2.0	7

ZHONGLIANG WANG

#	Article	IF	CITATIONS
19	Rabies Virusâ€Inspired Metal–Organic Frameworks (MOFs) for Targeted Imaging and Chemotherapy of Glioma. Angewandte Chemie - International Edition, 2020, 59, 16982-16988.	13.8	53
20	An activatable liposomal fluorescence probe based on fluorescence resonance energy transfer and aggregation induced emission effect for sensitive tumor imaging. Colloids and Surfaces B: Biointerfaces, 2020, 188, 110789.	5.0	5
21	A pH ratiometrically responsive surface enhanced resonance Raman scattering probe for tumor acidic margin delineation and image-guided surgery. Chemical Science, 2020, 11, 4397-4402.	7.4	25
22	RNA-silencing nanoprobes for effective activation and dynamic imaging of neural stem cell differentiation. Theranostics, 2019, 9, 5386-5395.	10.0	6
23	Highly Stable and Longâ€Circulating Metalâ€Organic Frameworks Nanoprobes for Sensitive Tumor Detection In Vivo. Advanced Healthcare Materials, 2019, 8, 1900761.	7.6	22
24	Liposome-based probes for molecular imaging: from basic research to the bedside. Nanoscale, 2019, 11, 5822-5838.	5.6	55
25	Toxic Reactive Oxygen Species Enhanced Synergistic Combination Therapy by Selfâ€Assembled Metalâ€Phenolic Network Nanoparticles. Advanced Materials, 2018, 30, 1704877.	21.0	311
26	Hypochlorous Acid Promoted Platinum Drug Chemotherapy by Myeloperoxidase-Encapsulated Therapeutic Metal Phenolic Nanoparticles. ACS Nano, 2018, 12, 455-463.	14.6	134
27	Development of functionalized gold nanoparticles as nanoflare probes for rapid detection of classical swine fever virus. Colloids and Surfaces B: Biointerfaces, 2018, 171, 110-114.	5.0	6
28	In Vivo and in Situ Activated Aggregation-Induced Emission Probes for Sensitive Tumor Imaging Using Tetraphenylethene-Functionalized Trimethincyanines-Encapsulated Liposomes. ACS Applied Materials & Interfaces, 2018, 10, 25146-25153.	8.0	34
29	Multifunctional Molecular Beacon Micelles for Intracellular mRNA Imaging and Synergistic Therapy in Multidrugâ€Resistant Cancer Cells. Advanced Functional Materials, 2017, 27, 1701027.	14.9	45
30	Recent advances in high-performance fluorescent and bioluminescent RNA imaging probes. Chemical Society Reviews, 2017, 46, 2824-2843.	38.1	118
31	Core–Shell Gold Nanorod@Metal–Organic Framework Nanoprobes for Multimodality Diagnosis of Glioma. Advanced Materials, 2017, 29, 1604381.	21.0	177
32	Improved Tumor Targeting and Longer Retention Time of NIR Fluorescent Probes Using Bioorthogonal Chemistry. Theranostics, 2017, 7, 3794-3802.	10.0	34
33	Activation of mesenchymal stem cells by macrophages promotes tumor progression through immune suppressive effects. Oncotarget, 2016, 7, 20934-20944.	1.8	45
34	Increased precision of orthotopic and metastatic breast cancer surgery guided by matrix metalloproteinase-activatable near-infrared fluorescence probes. Scientific Reports, 2015, 5, 14197.	3.3	27
35	Smart MoS ₂ /Fe ₃ O ₄ Nanotheranostic for Magnetically Targeted Photothermal Therapy Guided by Magnetic Resonance/Photoacoustic Imaging. Theranostics, 2015, 5, 931-945.	10.0	234
36	In vivo nanoparticle-mediated radiopharmaceutical-excited fluorescence molecular imaging. Nature Communications, 2015, 6, 7560.	12.8	114

ZHONGLIANG WANG

#	Article	IF	CITATIONS
37	Engineered Mesenchymal Stem Cells with Enhanced Tropism and Paracrine Secretion of Cytokines and Growth Factors to Treat Traumatic Brain Injury. Stem Cells, 2015, 33, 456-467.	3.2	74
38	Zoledronic acid prevents the tumor-promoting effects of mesenchymal stem cells via MCP-1 dependent recruitment of macrophages. Oncotarget, 2015, 6, 26018-26028.	1.8	30
39	Bioinspired Nanocomplex for Spatiotemporal Imaging of Sequential mRNA Expression in Differentiating Neural Stem Cells. ACS Nano, 2014, 8, 12386-12396.	14.6	27
40	Biomimetic RNAâ€Silencing Nanocomplexes: Overcoming Multidrug Resistance in Cancer Cells. Angewandte Chemie - International Edition, 2014, 53, 1997-2001.	13.8	55
41	Glucose Oxidase-Catalyzed Growth of Gold Nanoparticles Enables Quantitative Detection of Attomolar Cancer Biomarkers. Analytical Chemistry, 2014, 86, 5800-5806.	6.5	160
42	Self-Assembled Colloidal Superparticles from Nanorods. Science, 2012, 338, 358-363.	12.6	332
43	Shape-Controlled Synthesis of Colloidal Superparticles from Nanocubes. Journal of the American Chemical Society, 2012, 134, 18225-18228.	13.7	121
44	Nanoparticle-based artificial RNA silencing machinery for antiviral therapy. Proceedings of the National Academy of Sciences of the United States of America, 2012, 109, 12387-12392.	7.1	63
45	One‣tep Selfâ€Assembly, Alignment, and Patterning of Organic Semiconductor Nanowires by Controlled Evaporation of Confined Microfluids. Angewandte Chemie - International Edition, 2011, 50, 2811-2815.	13.8	70
46	Chemically responsive luminescent switching in transparent flexible self-supporting [EuW ₁₀ 0 ₃₆] ^{9â^'} -agarose nanocomposite thin films. Journal of Materials Chemistry, 2010, 20, 271-277.	6.7	85
47	Transparent and flexible phosphomolybdate–agarose composite thin films with visible-light photochromism. Journal of Materials Chemistry, 2010, 20, 1107-1111.	6.7	47
48	Reversible Luminescent Switching in a [Eu(SiW ₁₀ MoO ₃₉) ₂] ^{13â^'} â€Agarose Composite Film by Photosensitive Intramolecular Energy Transfer. Advanced Materials, 2009, 21, 1737-1741.	21.0	85
49	Fabrication of self-assembled ultrathin photochromic films containing mixed-addenda polyoxometalates H5[PMo10V2O40] and 1,10-decanediamine. Journal of Solid State Chemistry, 2009, 182, 983-988.	2.9	22
50	Effects of Photoinduced Electron Transfer on the Rational Design of Molecular Fluorescence Switch. Journal of Physical Chemistry C, 2009, 113, 2594-2602.	3.1	26
51	Superhydrophobic pure silver surface with flower-like structures by a facile galvanic exchange reaction with [Ag(NH3)2]OH. Chemical Communications, 2008, , 2692.	4.1	35
52	A Novel Redox-Fluorescence Switch Based on a Triad Containing Ferrocene and Perylene Diimide Units. Organic Letters, 2008, 10, 3065-3068.	4.6	104
53	Intercalation and Photophysical Properties of the Tetra-(8-hydroxyquinolinato) Boron Complex and 3,3â€~,4,4â€~-Benzophenone Tetracarboxylic Anion into Mgâ°'Al Layered Double Hydroxides. Inorganic Chemistry, 2006, 45, 4364-4371.	4.0	38
54	Synthesis and properties of Mg2Al layered double hydroxides containing 5-fluorouracil. Journal of Solid State Chemistry, 2005, 178, 736-741.	2.9	111

#	Article	IF	CITATIONS
55	Novel hydrogen-bonded three-dimensional network complexes containing copper-pyridine-2,6-dicarboxylic acid. Journal of Coordination Chemistry, 2004, 57, 1353-1359.	2.2	11
56	Synthesis and characterization of ultrathin multilayer films based onÂmolybdenum polyoxometalate (Mo54)n. Journal of Colloid and Interface Science, 2004, 274, 602-606.	9.4	8